International Journal of Powertrains

ISSN online: 1742-4275 - ISSN print: 1742-4267
https://www.inderscience.com/ijpt

Design and implementation of novel variants of multi-level inverters for traction and heavy vehicle applications

S. Sri Krishna Kumar, P.K. Dhal

DOI: 10.1504/IJPT.2023.10054774

Article History:

Received:	24 November 2021
Accepted:	31 May 2022
Published online:	20 March 2023

Design and implementation of novel variants of multi-level inverters for traction and heavy vehicle applications

S. Sri Krishna Kumar* and P.K. Dhal

Department of Electrical and Electronics Engineering,
Vel Tech Rangarajan Dr. Sagunthala
R&D Institute of Science and Technology,
Chennai, India
Email: kkumarveltech@gmail.com
Email: krishnakumar.rvs@gmail.com
Email: pradyumna.dhal@rediffmail.com
Email: pkdhal64@yahoo.com
*Corresponding author

Abstract: In the advent of increased transportation systems, the importance and growth of heavy vehicle movements and their applications play a significant role. The transportation sector involving heavy vehicles needs appropriate components for systematic movements. With the prominence of components utilised in heavy vehicle systems and power train mechanism, this paper develops novel variants of multi-level inverters for effective functioning of the vehicular system. Along with the classic multi-level inverter (MLI), new variants – modified multi-level inverter and reduced switch multi-level inverter are designed with complete operation based on their switching states and are implemented for a nine level output voltage module. The proposed inverter models for the heavy vehicle system is tested and validated based on the total harmonic distortion (THD). For each level and their switching states, THD is evaluated and the inverter performance is proved for its superiority for heavy vehicle system and their applicability in power train applications.

Keywords: heavy vehicle system; component design; multi-level inverter; MLI; reduced switch multi-level inverter; total harmonic distortion; THD; switching states; power trains; duty cycle; switching losses; power quality.

Reference to this paper should be made as follows: Kumar, S.S.K. and Dhal, P.K. (2023) 'Design and implementation of novel variants of multi-level inverters for traction and heavy vehicle applications', *Int. J. Powertrains*, Vol. 12, No. 1, pp.54–80.

Biographical notes: S. Sri Krishna Kumar has completed his graduation in Electrical and Electronics Engineering from RVSCET, Dindigul under Anna University during 2008, and post-graduation in Power Electronics and Drives from Government College of Engineering, Salem under Anna University during 2011. He has teaching experience of nearly ten years in engineering colleges. His current area of research includes power electronic converters, power electronic applications to power system, circuit analysis for power electronic circuits. He holds a life membership in professional society IAENG, ICST, EAI (eu), ISTE.

P.K. Dhal received his ME degree in Power Systems from Madurai Kamaraj University in 2002, Madurai, India. He received his PhD in Power System from Sathyabama University., Chennai, India in 2014. He published technical papers in international and national journals and conferences. He is currently working as a Professor of Electrical and Electronics Engineering Department at Vel Tech Rangarajan Dr. Sagunthala R&D Institute of Science and Technology, Chennai, India. His areas of interest are power system optimisation, power quality and power system application to power electronics. He acquired membership in ISTE and IEEE in India.

1 Introduction

With the growth of heavy duty commercial vehicles, the requirement and application of inverters are most significant and design and implementation of these power electronic circuits for switching larger range of currents like 1,000 amperes with a fraction of microseconds are a herculean task for each engineer working in this domain area. The design of new variants of inverters adopts to minimise the stray inductances and as well ensures to achieve appropriate current sharing. In the current scenario with the minimise cost of power semiconductor devices and increased price of other components, the design of inverters in an optimal way is more essential. Utilising the electrical power for multiple applications like power train systems, heavy vehicle system and electric vehicle (EV) systems and other industrial and domestic purposes has resulted in the development of power modulating circuits. The existing limitation of these circuits lies in its capacity of identifying the proper circuit and topology. Power electronics based design strategy is one of the promising fields to address the existing complexities in circuitry and making it more suitable for heavy vehicle and power train systems.

Inverter is the heart of any vehicle system, any power trains, EVs, hybrid electric vehicle (HEVs), heavy duty commercial vehicles and so on, as it drives the electrical power across the battery, electric motor, on-board charger and other electric circuitry. The power transistors and diodes of the inverters tend to pump electrons in and out of the electrical circuits of the vehicle system designed. In this case, the voltage level has to be maintained appropriately and at a suitable level so as to synchronise the movement of the vehicle properly. Airliner and HEV is the sweeping change in the case of utilisation of high frequency. Here the power frequency is said to be the output frequency, which is the number of cycles per second. Another frequency term used is the switching frequency, which is defined by the interval within the bounds of ON and OFF time of the switches. Figure 1 provides the basic components of heavy vehicle systems with the inverter configuration.

The significant importance of inverter is that, when the inverter of a heavy duty vehicle can support a higher voltage, the respective voltage charging current is larger and subsequently power is larger, meaning that the same current is charged, and the charging power gets scaled up and the charging time is minimised. When the support voltage of the inverter becomes higher, then the heat generated by the inverter at that particular charging gets increased and thus efforts has also to be taken for solving the heat dissipation problem of the inverter model and as well the charging efficiency of the model has to be improved. In the inverter module, more heat gets released on increasing

the switching frequency and since the design of inverter is highly complex, its transient thermal characteristics have to be captured accurately. Due to which, this research study is intended to model and implement the inverter models so as to operate and deliver the most highest efficiency in the heavy vehicle and power train system design.

Figure 1 Basic configuration, (a) simple EV module, (b) heavy vehicle system (see online version for colours)

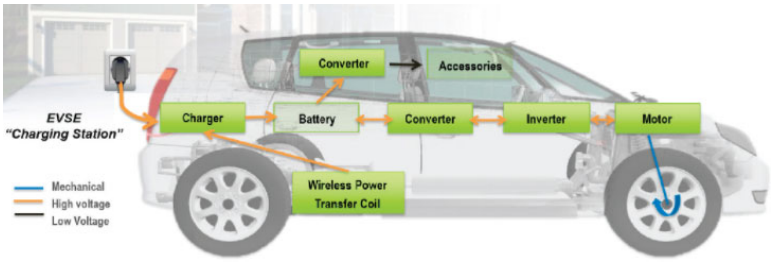

(a)

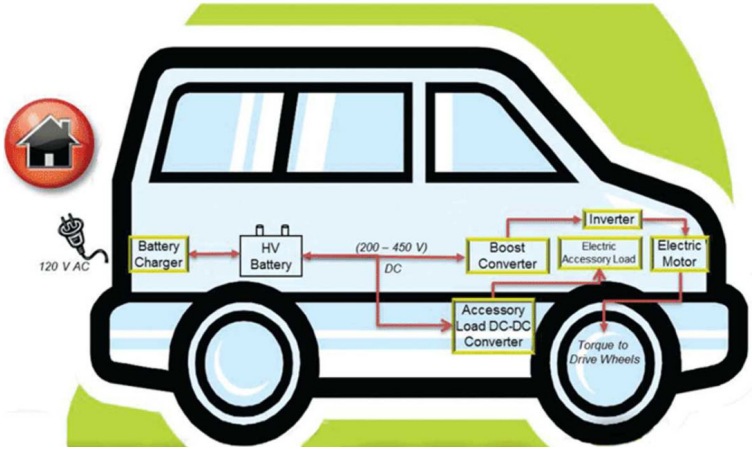

(b)

2 Related works

Over the past few years numerous works have been carried out for design of various forms of inverters for EVs, hybrid EVs, heavy duty commercial vehicles and other related power train system modules. In each and every design, attempt is taken for better charging efficiency of the inverter model and its withstanding capacity during various operating conditions. Hence, this design and modelling of inverters for vehicle applications is always a thrust area for researchers and industry professionals. This section of the research study presents related works carried out in the field of inverter design for heavy vehicle applications.

Luniewski and Jansen (2007) explained the importance and applicability of high level inverters and their usage in heavy vehicle systems. In a work by Xiu-Juan et al. (2008), the inverter's performance has been improved by placing voltage-rising section in the

DC-DC previous section, and by replacing fundamental frequency transformer with high frequency transformer, thereby, the inverter's size and weight is reduced at the same time. Wu et al. (2010) carried out modelling and design method of electrical drive and power inverter applied to a powertrain for a heavy duty series-parallel HEV.

Desai et al. (2012) developed IGBT power modules and inverters used in VOLTec and eAssist, and carried out power modules reliability tests; power cycle, intermittent operation life and thermal air shock tests. Drobnik and Jain (2013) concentrated on a small to medium size personal vehicles in EV and parallel hybrid (HEV) configuration. Even though the main focus of the paper was the traction inverter, other critical high power EV and HEV building blocks such as a DC/DC and AC/DC on board charger were also characterised. Murthy-Bellur et al. (2015) introduced the use of power electronics in power generation and vehicle electrification applications. Using examples, potential use of WBG semiconductors in these applications were discussed.

Kumar et al. (2015) investigated the effect of increase in levels from 3 to 33 levels, using a simplified technique in separate source cascaded multilevel inverter (CMlI) on the total harmonic distortion (THD) for 1-phase and 3-phase inverter without using any filters. Schwalbe and Schilling (2015) focussed on the topology-optimisation of a 25 kW modular machine-inverter drive train system for EVs, hybrid vehicles (48 V system) or industrial trucks (e.g., fork lifters). The consequence of the detected optimal battery voltage level and the analysis of the system power loss distribution was the development of new drive train power topologies. Sun et al. (2016) modelled a control strategy for a bridge inverter module and it was capable of handling the short circuit fault of the EV integrated drive system. Yamaguchi et al. (2017) presented detailed study on the various variants of the developed hybridised heavy duty vehicles.

Chen et al. (2015) improved dynamic performance and reliability of the droop method by improving power calculation and introducing the whole cycle adaptive droop method in auxiliary inverters. Youssef et al. (2015) presented a new trend in the transportation industry to adopt the multilevel inverter-based propulsion systems and gives the design procedure of a new dc/ac three-phase six-level inverter for powering the rail metro cars. Jeschke et al. (2016) developed a passive load, modelling the impedance behaviour of an existing motor. Thus no bushing and no setup for load torque generation has to be used for drive inverters test setup according to CISPR 25. Ye et al. (2017) proposed a configuration method for inverter feedback device has been proposed based on multi-train operation and traction power supply simulation. In order to ensure the safety of traction power supply, the train network voltage and rail potential are considered.

Wang et al. (2017) proposed a method based on the inverter output frequency compensation by detecting DC side voltage, resulting in controlling the energy state and suppress induction motor load oscillation. Zhong et al. (2018) utilised inverter and motor overload capabilities to improve motor braking in high speed areas. Moreover, the losses of the DC side, inverter and motor are analysed for the actual parameters of Beijing Metro. Nakanishi et al. (2018) focused on presenting the benefits of a newly developed SiC power module and the utilisation of this module in a power train inverter.

Namiki et al. (2018) modelled a new inverter power module that adopts a direct cooling structure produces higher current density than the previous model. The designs of components experiencing structural and electrical variation that affects heat generation by the power semiconductors were confirmed. Sooraj and Febin Daya (2018) proposed a

modified class E converter topology for an efficient power transfer application at lower switching frequency compared to the class E wireless power transfer (WPT) system. The converter uses minimum semiconductor switches to perform the inverter action, thereby reducing the cost and making the IPT system more compact. Chen and Ge (2018) investigated high power traction inverter design, from a practical point of view, through providing three options for EV applications.

Wang et al. (2018) proposed a holistic power electronic circuits design to achieve 4 × power density at 98% peak efficiency for a compact 250 kW three-phase three-level (3-L) T-type traction inverter. The proposed T-type inverter is designed using the best in class silicon carbide (SiC) power modules. Ji et al. (2018) adapted a current-enhanced inverter topology with auxiliary network to design a wide-power-range inverter for wireless charging system. Dorn-Gomba et al. (2019) introduced the concept of the multi-source inverter as an alternative solution to reduce the power rating of the dc-dc converter while keeping similar powertrain performance. The implementation of the multi-source inverter in a hybrid power-split powertrain is discussed in this work.

Anwar et al. (2020) presented an automated controller for an integrated, reconfigurable dc-dc converter for plug-in EVs. The automated controller selects the operating mode and inverter bus voltage at different torque-speed conditions to get maximum overall traction drive efficiency. Gopi and Babu (2021) developed an electronic differential controller (EDC), which replaces the traditional heavy and lossy mechanical differential present in an EV inverter system. Feng et al. (2021) presented the design of a high-performance SPM machine without any heavy rare-earth material that was optimised specifically for a current-source inverter (CSI) traction drive. This machine was designed for a constant-power speed ratio (CPSR) of 3.

Zhang et al. (2019) developed a simplified power system model containing regenerative inverters and trains. The inverter operating characteristics were optimised by a cost function considering total energy consumption, brake shoes wear, and inverter expense. Krim et al. (2020) focused on the improving of the energy efficiency of electrical train in braking mode and the improvement has been explored by integration and control of a reversible inverter in a DC power substation to inject the braking power from the DC railway electrical network to the AC transmission grid. Li et al. (2021) modelled a type of 3.3-kV/450-A half-bridge insulated-gate bipolar transistor (IGBT) power module combining the silicon (Si) and silicon carbide (SiC) technologies, for the miniaturisation of the Chinese high-speed railway rolling stock traction inverters.

Wang and Lehn (2021) presented a three-phase EV charger integrated with the dual inverter drive. Integrated charging can substantially reduce charging station costs by reemploying drivetrain components. Schweikert et al. (2021) built the silicon carbide [SiC] based, air-cooled traction inverter and tested for a mid-sized passenger vehicle. This work described the inverter's electrical and thermal concept, the first test results and provides an outlook to the proposed next steps. Zhang et al. (2021) developed drive boards on DKZ31 metro, and carried out the test work. On the basis of ensuring the safety and reliability, the maintenance cost is greatly reduced and the maintenance efficiency is improved with the inverter design.

Wu et al. (2020) for evaluating the weak links and various components performance and ascertain the effect of high temperature on the traction inverter, the traction inverter HALT was carried out with higherature stress between 190°C–220°C taking the IGBT on-die temperature as the benchmark. Jayal and Bhuvaneswari (2021) explored the reduced switch five-level transistor – clamped H bridge (TCHB) inverter topology for

driving a PMSM, particularly for an EV application. The TCHB inverter emulates the modular structure of a cascaded H bridge (CHB) inverter, with each phase being energised by independent DC sources, thereby making it a natural fit for EVs. Blaabjerg et al. (2021) discussed the reliability-oriented design methodology with an EV onboard charger and the drive train inverter.

From the extensive literature made on the existing works, the limitations with respect to the design of inverter are observed as:

- Large amount of heat being generated by the power semiconductor devices (Sun et al., 2016; Yamaguchi et al., 2017; Chen et al., 2015; Youssef et al., 2015; Jeschke et al., 2016; Ye et al., 2017).
- Not at ease in managing the electric drive system (Drobnik and Jain, 2013; Murthy-Bellur et al., 2015; Kumar et al., 2015; Schwalbe and Schilling, 2015).
- Certain voltage source inverters (VSIs) result in big inverter ripple (Wang et al., 2017, 2018; Zhong et al., 2018; Nakanishi et al., 2018; Namiki et al., 2018; Sooraj and Febin Daya, 2018; Chen and Ge, 2018; Ji et al., 2018; Dorn-Gomba et al., 2019).
- Large inductor when the output frequency is low in VSI (Anwar et al., 2020).
- Micro inverters developed have the problem with the employed solar panel, and fault rectification seems to be time consuming (Gopi and Babu, 2021; Feng et al., 2021; Zhang et al., 2019; Krim et al., 2020; Li et al., 2021; Wang and Lehn, 2021).
- High cost involved in micro inverters and difficulty encountered in their maintenance (Schweikert et al., 2021).
- Power production of the system gets drastically decreased with a series inverter (Zhang et al., 2021; Wu et al., 2020; Jayal and Bhuvaneswari, 2021).
- Few inverters possess poor flexibility at partial shading (Blaabjerg et al., 2020).

In this research study, attempts are taken to overcome the above noted demerits of few existing inverter models and thereby focussed on developing inverters such that they:

- Can achieve better voltage output (waveform).
- Reduction in the switching frequency.
- Generation of high voltage employing low voltage sources.
- Designing multi-level inverters (MLIs) with several switches such that each switch gets involved in developing small level of voltage and as well controls the current for a minimum possible extent.
- Minimised level of harmonics.
- Smaller filter size is sufficient here to remove the minimal amount of harmonics.
- Improvement in the power quality of the system.
- THD is to be reduced due to the smooth output voltage waveform.
- Minimised switching losses.

The research study for efficient operation of the heavy vehicle applications intends to

- Design and develop a modified MLI with better minimised THD and significant improvement in the power quality.
- Modelling a new reduced switch MLI for effective operation of a power train and a heavy vehicle application system.

3 Methods and materials

In heavy vehicle applications and power train models, inverters are a kind of power modulating device which provides the solution to obtain alternating current when direct current is available. The development of inverter topologies has revolutionised the EVs, hybrid EVS, heavy duty vehicles and power train based traction modules. Always it is important to have quality power and inverter is one of the sources for the same. Due to which, in the development of heavy duty vehicles and EVs, researchers adopt different topologies varying in the configuration, control methodology and the quality of output power. The rise of computers and other semiconductor-based devices always introduces a drastic change in power quality throughout the development of inverters for EVs, power train and heavy vehicle applications.

3.1 Configuration of classic MLI for power train and heavy vehicle applications

Many different categories of inverters are commonly employed for power train and heavy duty commercial vehicles nowadays. Basically, the classic inverter models come under the category of VSI and current source inverter (CSI) (Anjali Krishna and Padma Suresh, 2016). Apart from these, inverters such as series inverter or parallel inverters are also designed and modelled. Variants of multilevel inverters exist with respect to their configuration and based on their circuit elements. The CMlI employs a series connection of H-bridge inverters and on the other hand, the Diode clamped inverters makes use of diodes along with the switches. The flying capacitor type inverters are of importance due to the presence of capacitor in the circuit. Further, hybrid inverters are also in the growing pace for power train models and this has paved the way towards the development of ultra-capacitors and capacitor banks.

Basic configuration of an inverter generally employed in EVs is the H-bridge inverter with four switches, which is a full bridge inverter circuit (Almakhles et al., 2020; Rashid, 2004; Guha and Narayanan, 2018; Choi and Sul, 1996; Shen and Jiang, 2019). Hence, such a bridge circuit provides the output with the peak voltage equal to the DC source connected. The two switches in each leg correspond to conduction either positive or output voltage to the load. Hence in each leg, the switches are named as positive switch and negative switch.

The switching pattern can be a fixed one or variable, depending on the vehicle application. Whatever the switching pattern, the switching is always managed by a microprocessor or a microcontroller (Hinago and Koizumi, 2010; Kumar et al., 2015; Nagalakshmi et al., 2017; Choi et al., 2018). Such devices operate at a low voltage, and the design standards restrict the output of such control structures to be minimal. But the power electronic switches need a higher control voltage, for gate drive or base drive and for this purpose driver circuits are employed, which amplifies the control signal to latch

the switches. Certain operations demanding higher frequency of signals also requires the data from controller to be stored temporarily or permanently. Such storage or buffer is also provided by the driver circuit. Also there arises a need to electrically isolate the low voltage control circuit from the higher voltage power circuit, which is satisfied by the driver circuit. Figure 2 illustrates the output waveform of an ideal MLI configuration.

Figure 2 Output waveform of ideal inverter model employed in EVs

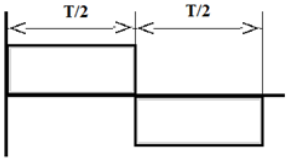

Considering a square wave output of an ideal inverter employed in EVs, as in Figure 2, the output can be derived using the expression given below,

$$V_{rms} = \sqrt[2]{\frac{1}{T}\left\{\int_0^T V_0^2 dt\right\}} \tag{1}$$

Due to symmetry, the interval 0 to T is split into equal parts for positive and negative half cycles. The entire interval is split as 0 to $\frac{T}{2}$ for positive half cycle and $\frac{T}{2}$ to T for the negative half cycle.

$$\begin{aligned} V_{rms} &= \sqrt[2]{\frac{1}{T}\left\{\int_0^{T/2} V_0^2 dt + \int_{T/2}^T V_0^2 dt\right\}} \\ &= \sqrt{\frac{1}{T}(V)^2\left(\frac{T}{2}-0\right)+(-V)^2\left(T-\frac{T}{2}\right)} \end{aligned} \tag{2}$$

$$V_{rms} = V \tag{3}$$

Figure 3 Output waveform of inverter model of EV with dead time

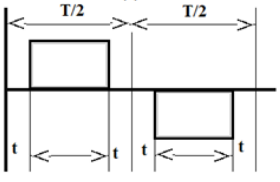

Considering an output of an ideal inverter with three levels, the output shown in Figure 3 is derived using the expression given below:

$$V_{rms} = \sqrt[2]{\frac{1}{T}\left\{\int_0^T V_0^2 dt\right\}} \tag{4}$$

Since the 3 stepped square wave experiences 0v for a small duration, the conduction duration is split into two half cycles with an equal dead time for both half cycles (Guha

and Narayanan, 2018; Choi and Sul, 1996). In other words, a duration of '*t*' for each half cycle gets included. The entire interval is split as 0 to $\frac{T}{2}$ for positive half cycle and $\frac{T}{2}$ to T for the negative half cycle. Further, 0 to $\frac{T}{2}$ is divided as 0 to t; t to $\frac{T}{2}-t$; $\frac{T}{2}-t$ to $\frac{T}{2}$. Similarly, $\frac{T}{2}$ be divided as $\frac{T}{2}$ to $\frac{T}{2}+t$; $\frac{T}{2}+t$ to $T-t$; $T-t$ to T.

$$V_{rms} = \sqrt[2]{\frac{1}{T}\left\{\int_0^{T/2} V_0^2 dt + \int_{T/2}^{T} V_0^2 dt\right\}} \tag{5}$$

$$\begin{aligned} V_{rms} &= \sqrt[2]{\frac{1}{T}\left\{\int_0^{t} V_0^2 dt + \int_t^{\frac{T}{2}-t} V_0^2 dt + \int_{\frac{T}{2}-t}^{T/2} V_0^2 dt + \int_{T/2}^{\frac{T}{2}+t;T} V_0^2 dt + \int_{\frac{T}{2}+t;}^{T-t} V_0^2 dt + \int_{T-t}^{T} V_0^2 dt\right\}} \\ &= \sqrt[2]{\frac{1}{2}\left\{\int_t^{\frac{T}{2}-t} V_0^2 dt + \int_{\frac{T}{2}+t;}^{T-t} V_0^2 dt\right\}} \end{aligned} \tag{6}$$

$$V_{rms} = \sqrt[2]{\frac{1}{T}\left\{(V)^2\left(\frac{T}{2}-t-t\right) + (-V)^2\left(T-t-\left[\frac{T}{2}+t\right]\right)\right\}} \tag{7}$$

$$\begin{aligned} V_{rms} &= \sqrt[2]{\frac{1}{T}\left\{(V)^2\left(\frac{T}{2}-t-t\right) + (-V)^2\left(T-t-\frac{T}{2}-t\right)\right\}} \\ &= \sqrt{\frac{1}{T}\left\{(V)^2(T-4t)\right\}} \end{aligned} \tag{8}$$

$$V_{rms} = V\sqrt{\frac{1}{T}\{(T-4t)\}} \tag{9}$$

Figure 4 Configuration of classic MLI for power train applications

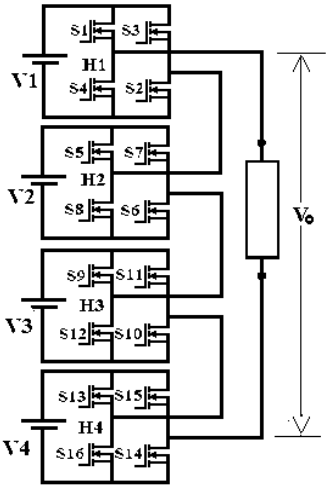

For the nine levels inverter the same output equation derived above is modified accordingly,

$$V_{rms} = V_1\sqrt{\frac{1}{T}\{(T-4t1)\}} + V_2\sqrt{\frac{1}{T}\{(T-4t2)\}} + V_3\sqrt{\frac{1}{T}\{(T-4t3)\}} + V_4\sqrt{\frac{1}{T}\{(T-4t4)\}} \tag{10}$$

The values of the non-conducting duration are given by; t_1 = 11.25°, t_2 = 33.75°, t_3 = 56.25°, t_4 = 78.75°. Considering the classic employed nine level output for heavy vehicle applications, all the output levels are at equal steps with symmetric waveform. Conventional multilevel inverter and reduced switch multilevel inverter illustrate a symmetric waveform whereas the modified multilevel inverter demonstrates an asymmetric waveform (António-Ferreira et al., 2018; Patil et al., 2018; Wang et al., 2018; Dong et al., 2018; Javvaji amd Basavaraja, 2013; Suresh and Panda, 2013). The peak voltage here is represented as 'V_{max}'. Table 1 provides the switching state of the classic MLI model. Figure 4 illustrates the configuration of the classic MLI design. Figure 5 presents the output waveform and conduction of classic MLI model.

Table 1 Switching state of classic MLI

Switches				*Output*
S1	*S2*	*S3*	*S4*	
1	1	0	0	+V
0	0	1	1	–V
0	0	0	0	0

Figure 5 Output waveform and conduction state of MLI in heavy vehicle and power train modules, (a) output waveform of classic MLI, (b) conduction state of classic MLI model (see online version for colours)

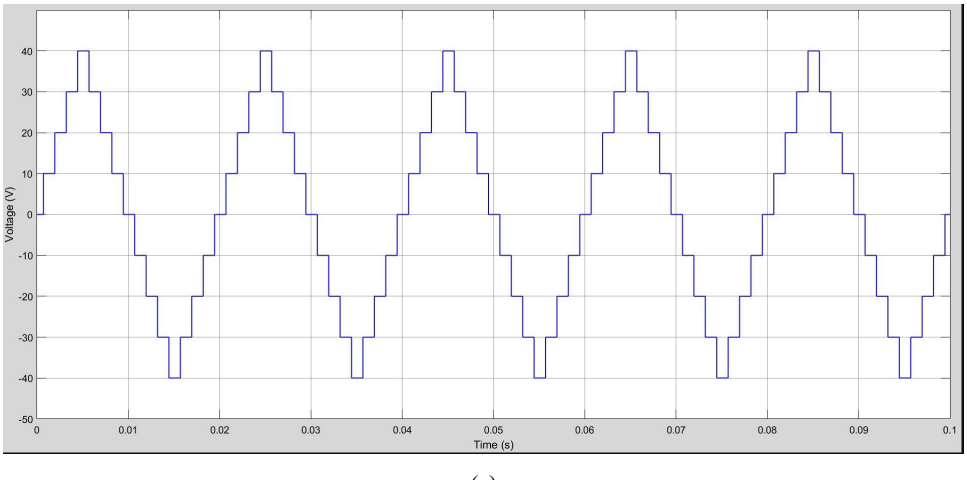

(a)

Figure 5 Output waveform and conduction state of MLI in heavy vehicle and power train modules, (a) output waveform of classic MLI, (b) conduction state of classic MLI model (continued) (see online version for colours)

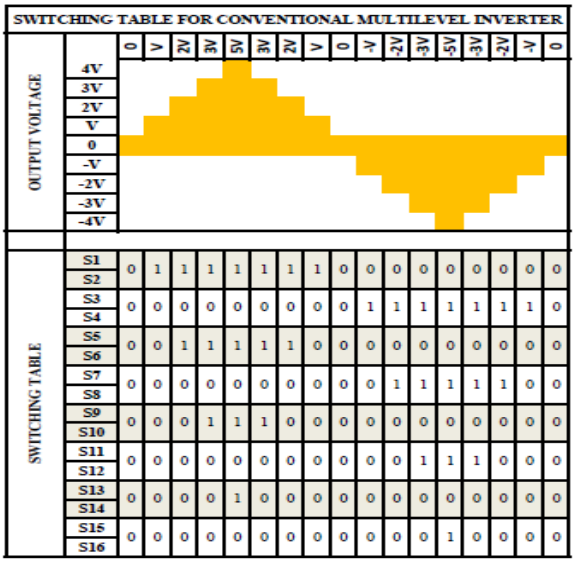

(b)

3.2 *Design of novel modified MLI for power train and heavy vehicle applications*

In the proposed novel MLI model for power train applications, multiple carrier schemes is employed and the required operation is carried out. An inverter connected in bridge configuration provides three distinct output voltages, namely 'V', '0', '–V'. While cascading the bridges, the input dc voltages are designed to be having the same magnitude. If the ratio between the input voltages are varied, then it gives way to obtain multiple output values, thereby breaking the conventional practice of using N bridges for 2N + 1 levels. Instead N number of bridges produces N2 output levels. Thus for obtaining nine levels, only two bridges are used whereas the traditional method makes use of four bridges. To obtain nine level output voltage, only 2 H-bridge inverters are connected in cascade as in Figure 6. The input dc voltages of the bridges are maintained at a ratio of 2:3.

Figure 6 New configuration of proposed modified MLI

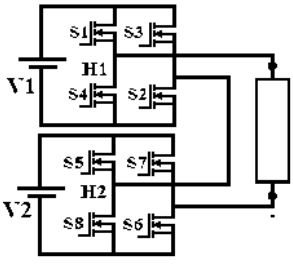

The output voltages are produced in individual bridges following the conventional multilevel inverter. The only difference is the duration and magnitude of the output voltages of individual bridges, which offers a difference in the cumulative output voltage. Figure 7 shows the variations of the current flow in the proposed modified MLI model.

Figure 7 Current flow variations of proposed modified MLI model, (a) current flow for +V, (b) current flow for –V, (c) current flow for +2V, (d) current flow for –2V, (e) current flow for +3V, (f) current flow for –3V, (g) current flow for +5V, (h) current flow for –5V

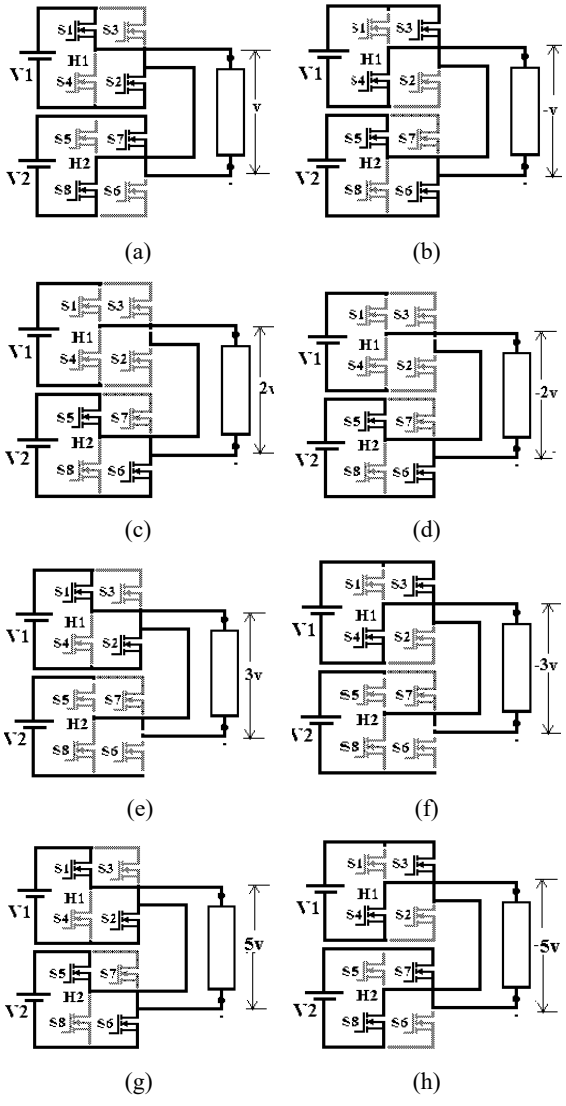

For the output voltage to be 'V' two bridges are allowed to conduct with *S1* and *S2* from *H1*, *S7* and *S8* from *H2* conducts. Here the bridge *H1* offers an output voltage of *3V* and *H2* offers *–2V*. Since the bridges are cascaded, the cumulative output obtained is *V* when

current flows through the path shown in Figure 7(a). Likewise, for the output voltage to be '*–V*', *S3* and *S4* from *H1*, and *S5* and *S6* from *H2* conducts. As in the positive cycle, the cumulative effect of *–3V* and *2V* provides an output of *–V* as shown in Figure 7(b). For the output voltage to be '*2V*' only one bridge *H2* is allowed to conduct with *S5* and *S6* turned on and in the same way, for the output voltage to be '*–2V*', *H2* is allowed to conduct, with *S7* and *S8* turned on as demonstrated in Figure 7(c) and Figure 7(d) respectively.

Figure 8 Implementation of proposed MLI in Simulink environment

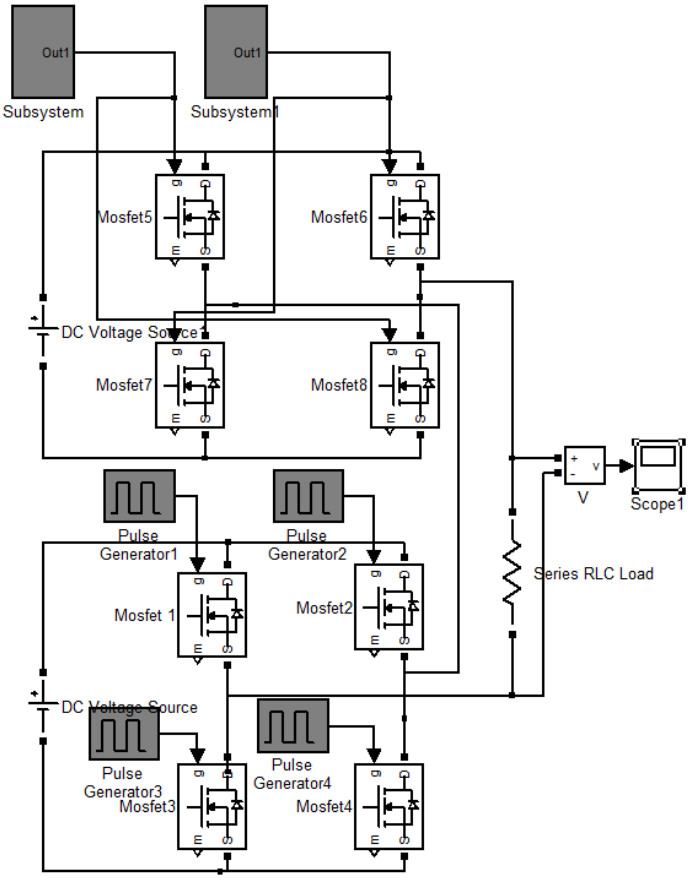

For the output voltage to be '*3V*' only one bridge H1 is allowed to conduct with *S1* and *S2* turned on as shown by Figure 7(e). Similarly, for the output voltage to be '*–3V*', *H1* is allowed to conduct, with *S3* and *S4* turned on as shown by Figure 7(f). Figure 7(g) and Figure 7(h) corresponds to the output voltages of '*5V*' and '*–5V*'. For the output voltage to be '*5V*' two bridges are allowed to conduct with *S1* and *S2* from *H1*, *S5* and *S6* from *H2* conducts. Here the bridge *H1* offers an output voltage of *3V* and *H2* offers *2V*. Since the bridges are cascaded, the cumulative output obtained is *5V*. Similarly, for the output voltage to be '*–5V*', *S3* and *S4* from *H1*, and *S7* and *S8* from *H2* conducts. As in the positive cycle, the cumulative effect of individual voltages *3V* and *2V* provides an output of *–5V*. Figure 8 demonstrates the implementation of the proposed modified MLI model

in MATLAB Simulink environment and Figure 9 depicts the output waveform and conduction state evaluated for the proposed new MLI model as applicable for the vehicle system applications.

Figure 9 Output waveform and conduction state of proposed modified MLI for vehicle system applications, (a) output waveform of new modified MLI (it smoothly follows the sine-wave characteristics), (b) conduction state of new MLI model (see online version for colours)

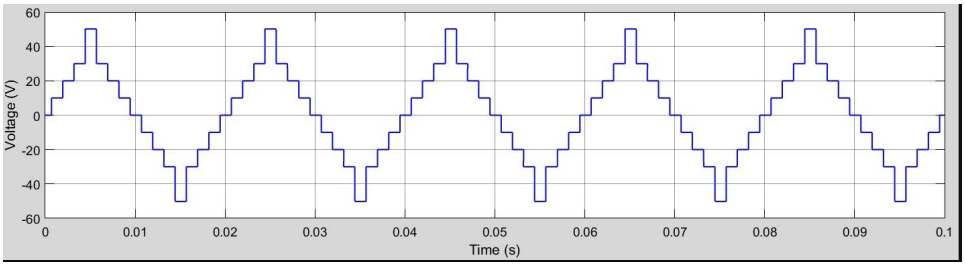

(a)

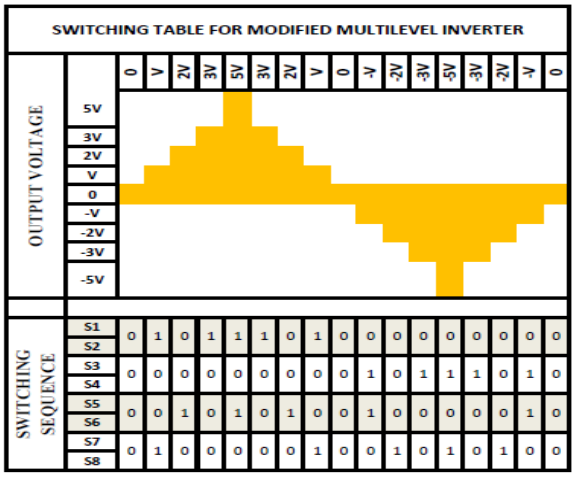

(b)

3.3 Design of new reduced switch MLI model for vehicle systems

In this research study, reduced switch multilevel inverter has been designed and implemented as a variant of the multilevel inverter topologies and this devised new topology operates with only one H-bridge. Additionally few switches are connected, which are termed as the auxiliary switches. The combinational switching of main and auxiliary circuits provides a multitude of outputs. Such an inverter designed for vehicle system applications is illustrated in Figure 10. Switch S2 from the main bridge and S7 from the auxiliary set conducts to connect one of the sources, V4, to the load. A positive voltage appears across the load. The current follows the path as, *Source*; *V4* (+) → *S7* → *Load* → *S2* → *Source*; *V4* (–). Similarly, S5 from auxiliary set and S3 from H-bridge

conduct to allow the load voltage and load current to be negative. Figure 11 presents the current flow variations of the proposed reduced switch MLI model.

Figure 10 Proposed reduced switch MLI model

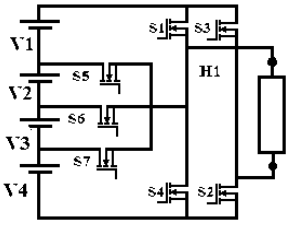

Figure 11 Current flow variations of proposed reduced switch MLI model, (a) current flow for +V (b) Current flow for –V, (c) current flow for +2V, (d) current flow for –2V, (e) current flow for +3V, (f) current flow for –3V, (g) current flow for +4V, (h) current flow for –4V

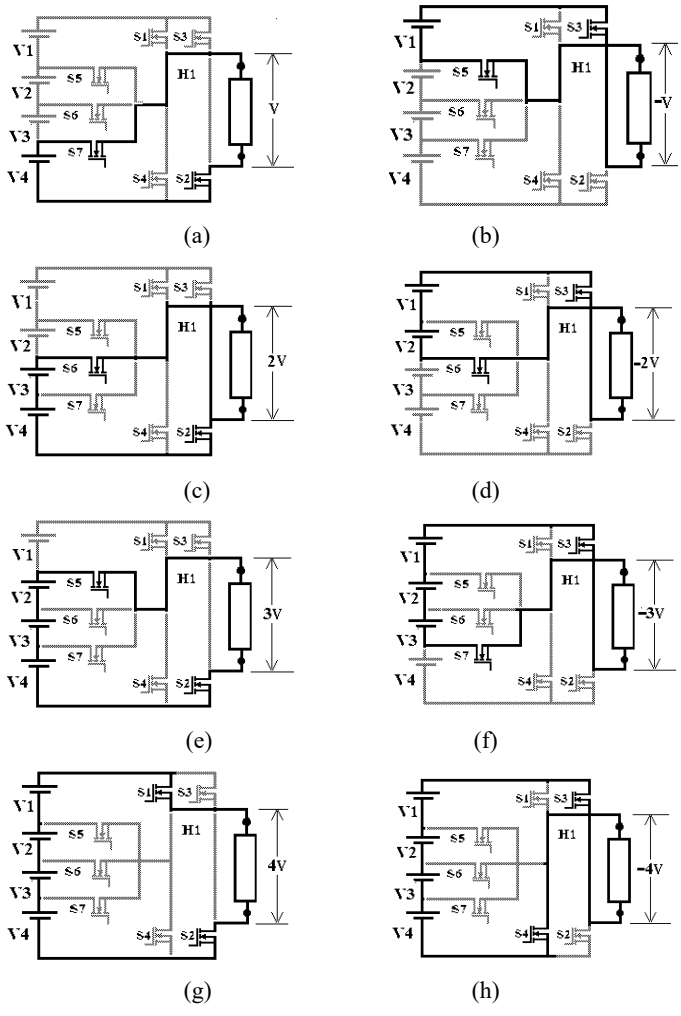

Figure 12 Implementation of proposed reduced switch MLI model

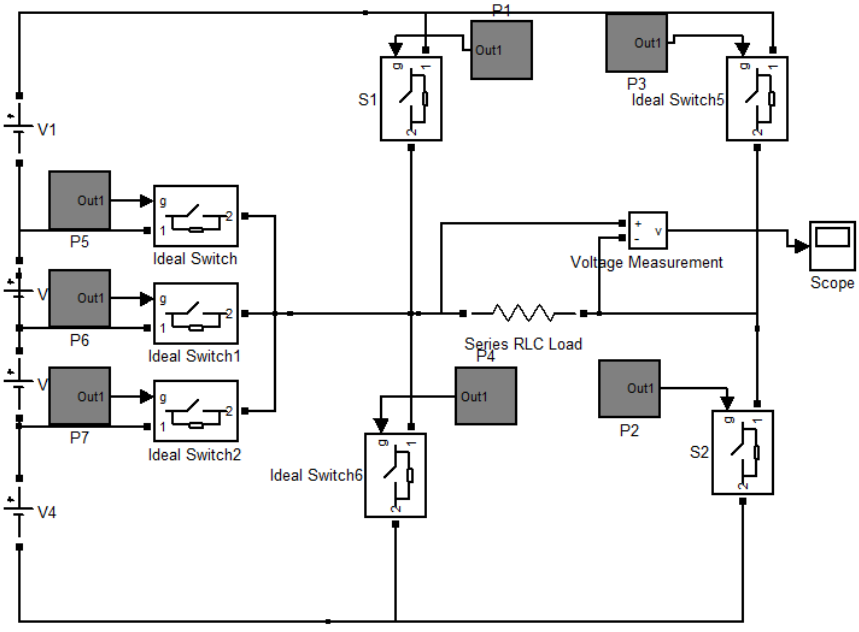

Current conduction as follows: *Source*, *V1* (–) → *S5* → *Load* → *S3* → *Source*, *V1* (+). Both these modes are shown in Figure 11(a) and Figure 11(b). Figure 11(c) shows switch S2 from the main bridge and S6 from the auxiliary set conduct to connect two sources, *V3* and *V4*, to the load. A positive voltage appears across the load. The current follows the path as, *Source*, *V3* and *V4* (+) → *S6* → *Load* → *S2* → *Source*, *V3* and *V4* (–). Similarly Figure 11(d) represents S6 from auxiliary set and S3 from H-bridge conducting to allow the load voltage and load current to be negative. Current conduction as follows: *Source*, *V1* and *V2* (+) → *S3* → *Load* → *S6* → *Source*, *V1* and *V2* (–). Switch S2 from the main bridge and S5 from the auxiliary set conducts to connect three of the sources, *V2*, *V3* and *V4*, to the load. A positive voltage appears across the load. The current follows the path as, *Source*: *V2*, *V3* and *V4* (+) → *S5* → *Load* → *S2* → *Source*: *V2*, *V3* and *V4* (–) as represented as in Figure 11(e). Similarly, S7 from auxiliary set and S3 from H-bridge conduct to allow the load voltage and load current to be negative. Current conduction is demonstrated by Figure 11(f) as: *V1*, *V2* and *V3* (+) → Si3 → *Load* → *S7* → *Source*, *V1*, *V2* and *V3* (–).

Switch *S1* and *S2* from the main bridge and none of the switches from the auxiliary set conducts to connect all the sources, *V1*, *V2*, *V3* and *V4*, to the load, shown by Figure 11(g). A positive voltage appears across the load. The current follows the path as, Source: *V1*, *V2*, *V3* and *V4* (+) → *S1* → *Load* → *S2* → *V1*, *V2*, *V3* and *V4* (–). Similarly, *S3* and *S4* from H-bridge conduct to allow the load voltage and load current to be negative as shown in Figure 11(h). Current conduction as follows: *V1*, *V2*, *V3* and *V4* (+) → *S3* → *Load* → *S4* → *Source*, *V1*, *V2*, *V3* and *V4* (–). The newly devised reduced switch inverter model is simulated as shown in Figure 12 and the respective output waveform and the conduction states of the new MLI model is presented in Figure 13. It is proven from the conduction states and the output waveform, that smooth waveform is obtained and this intends to reduce the distortions.

Figure 13 Output waveform and conduction state of proposed reduced switch MLI model, (a) output waveform of new reduced switch MLI model, (b) conduction state of new reduced switch MLI model (see online version for colours)

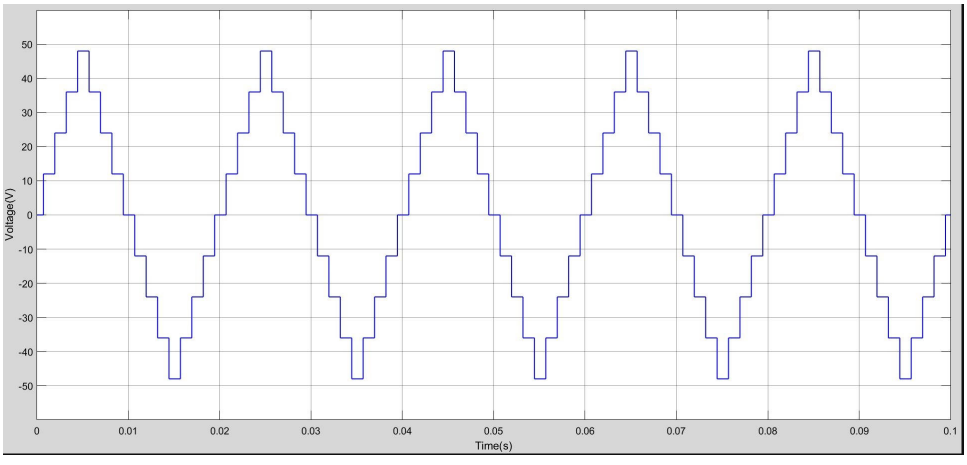

(a)

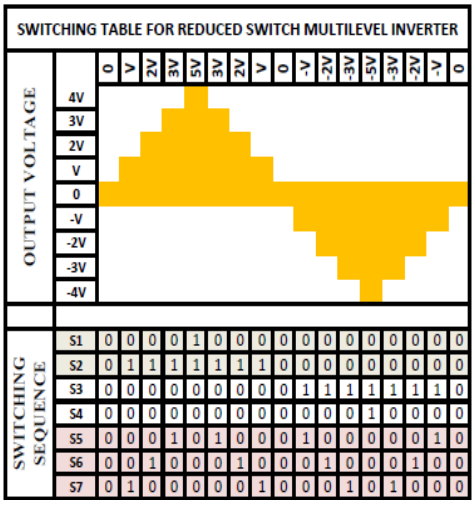

(b)

4 Results and comparative analysis

The two proposed MLIs – modified MLI and reduced switch MLI model as to be suited for power train and heavy vehicle design applications are tested for their superiority by evaluating their duty cycles and THDs. Both proposed MLI models and the classic MLI are analysed based on their response to their harmonics and their respective duty cycles of the individual switches. Generally, duty cycle is computed as the ratio between the duration of the switch being kept on in a cycle and the total duration of each cycle. Classic MLI model operates with four bridge circuits, comprising a total of 16 switches

and the switches in each of the bridges have a specific duty cycle. It shall be noted that each bridge have a unique duty cycle value. Table 2 lists the details pertaining to the classic MLI, proposed modified MLI model and reduced switch MLI model with respect to the number of switches used and their evaluated duty cycles.

Table 2 Duty cycle comparison of proposed MLI models employed for power train system

Proposed inverter models	*H-bridges*	*Switches*	*Conduction duration in each cycle*	*Evaluated duty cycle*
Classic multi-level inverter model	H1	S1	157.5	43.75
		S2		
		S3		
		S4		
	H2	S5	112.5	31.25
		S6		
		S7		
		S8		
	H3	S9	67.5	18.75
		S10		
		S11		
		S12		
	H4	S13	22.5	6.25
		S14		
		S15		
		S16		
Proposed modified MLI model	H1	S1	112.5	31.25
		S2		
		S3	112.5	31.25
		S4		
	H2	S5	112.5	31.25
		S6		
		S7	112.5	31.25
		S8		
Proposed reduced switch MLI model	H1 (main bridge)	S1	22.5	6.25
		S2	157.5	43.75
		S3	157.5	43.75
		S4	22.5	6.25
	Auxiliary circuit	S5	90	25
		S6	90	25
		S7	90	25

The designed modified multilevel inverter operates with eight switches as two H-bridges connected in cascade. All the switches are switched with same duty cycle but with different durations. The modelled reduced switch inverter configuration operates with

one bridge circuit and a set of auxiliary switches. Here for nine level output, three switches are connected as auxiliary set. Hence a total of seven switches are used. The bridge circuit and the auxiliary circuit have different duty cycle values. All the switches in the auxiliary circuit conduct at different duration in different combinations, yet they operate at same duty cycle. The switches in H-bridge, on the other hand, experiences different duty cycles. One switch for positive cycle and one for the negative cycle, namely S2 and S3 respectively, operates for major portion of each half cycle. The other two switches in the main bridge circuit, S1 and S4, operate at the least duty cycle, merely contributing only at the peak output voltage. All these observations are well inferred from the evaluated duty cycle presented in Table 2.

4.1 Comparison of proposed MLI models for low level loads

The proposed MLI models along with the classic MLI model for nine level outputs are analysed and the evaluated THD value is given in this section for low level loads (up to 10 W). Loads below 10 W considered here includes the R-load and RL-load and Figure 14 provides the graphical illustration of the attained THD value for the varying loads in respect of classic MLI, modified MLI and reduced switch MLI model.

Figure 14 Evaluation of THD for the proposed MLI models, (a) classic MLI model – R load, (b) classic MLI model – RL load, (c) proposed modified MLI model – R load, (d) proposed modified MLI model – RL load, (e) proposed reduced switch MLI model – R load, (f) proposed reduced switch MLI model – RL load (see online version for colours)

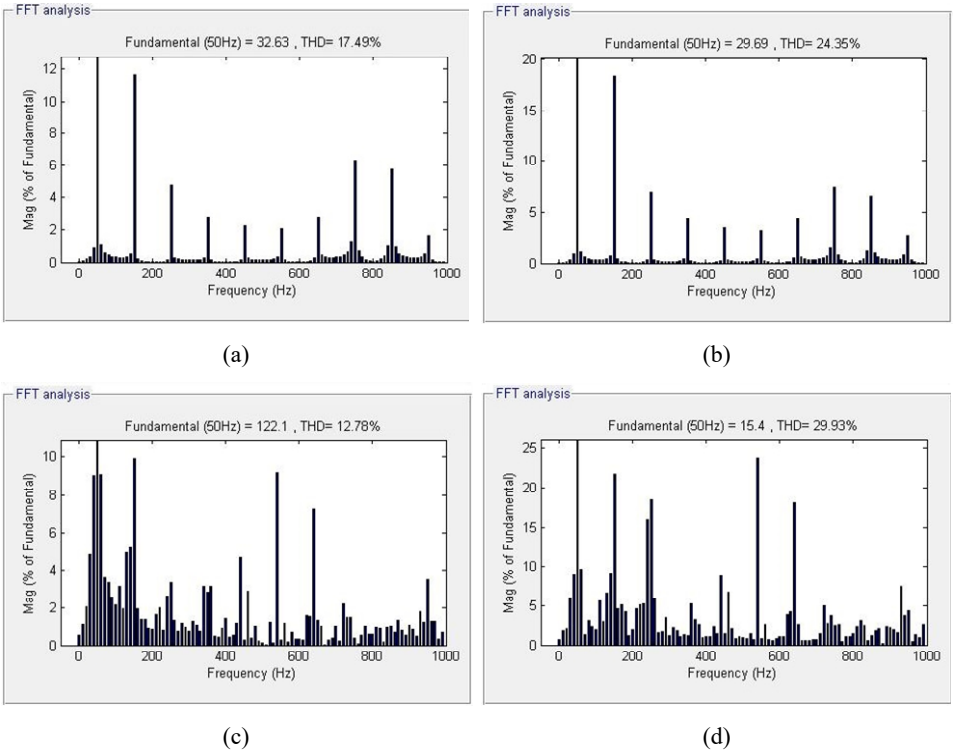

Figure 14 Evaluation of THD for the proposed MLI models, (a) classic MLI model – R load, (b) classic MLI model – RL load, (c) proposed modified MLI model – R load, (d) proposed modified MLI model – RL load, (e) proposed reduced switch MLI model – R load, (f) proposed reduced switch MLI model – RL load (continued) (see online version for colours)

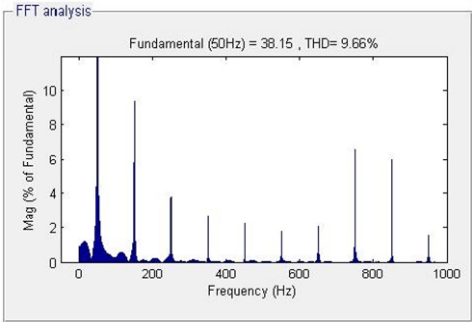

(e)

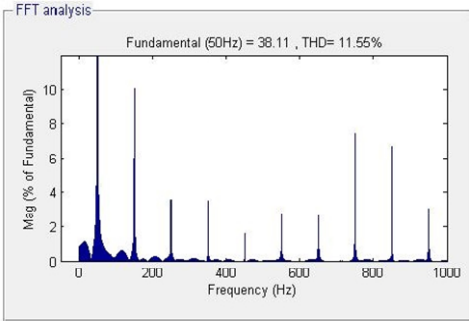

(f)

Table 3 lists the computed THD for the proposed MLI models for the R-loads and RL-loads. It is proven that the THD value is significantly minimised in respect of the proposed reduced switch MLI model than the modified MLI model and the classic MLI model as applicable for the power train applications. The significant reduction in the value of THD confirms that the better power quality is rendered by the inverter models for the power train applications.

Table 3 THD for low level loads of proposed MLI models

Proposed inverter configuration	*Load provided*	*Computed THD*
Classic MLI model	R	17.49
	RL	24.35
Modified MLI model	R	12.78
	RL	29.93
Reduced switch multilevel inverter model	R	9.66
	RL	11.55

4.2 Comparison of proposed MLI models for medium and high level loads

In this research study, the developed inverter models are verified for their THD values under medium (10 W to 50 W) and high load conditions (greater than 50 W), wherein certain power train applications shall require higher output voltage. Table 4 lists the evaluated THD value for medium and high load conditions and is inferred that out of all the proposed MLI models, reduced switch MLI model has yielded minimal THD under both medium and high load conditions. Figure 15 presents the THD evaluation for high load condition of the developed new MLI models. The reduction of THD is observed with reduced switch MLI model due to minimised switching states and duty cycle minimised to a most possible extent than the other two MLI models. This results in achieving better output voltage and increase the efficiency of charging the power train and heavy vehicle system applications.

Figure 15 Evaluation of THD for the proposed MLI models (high load)

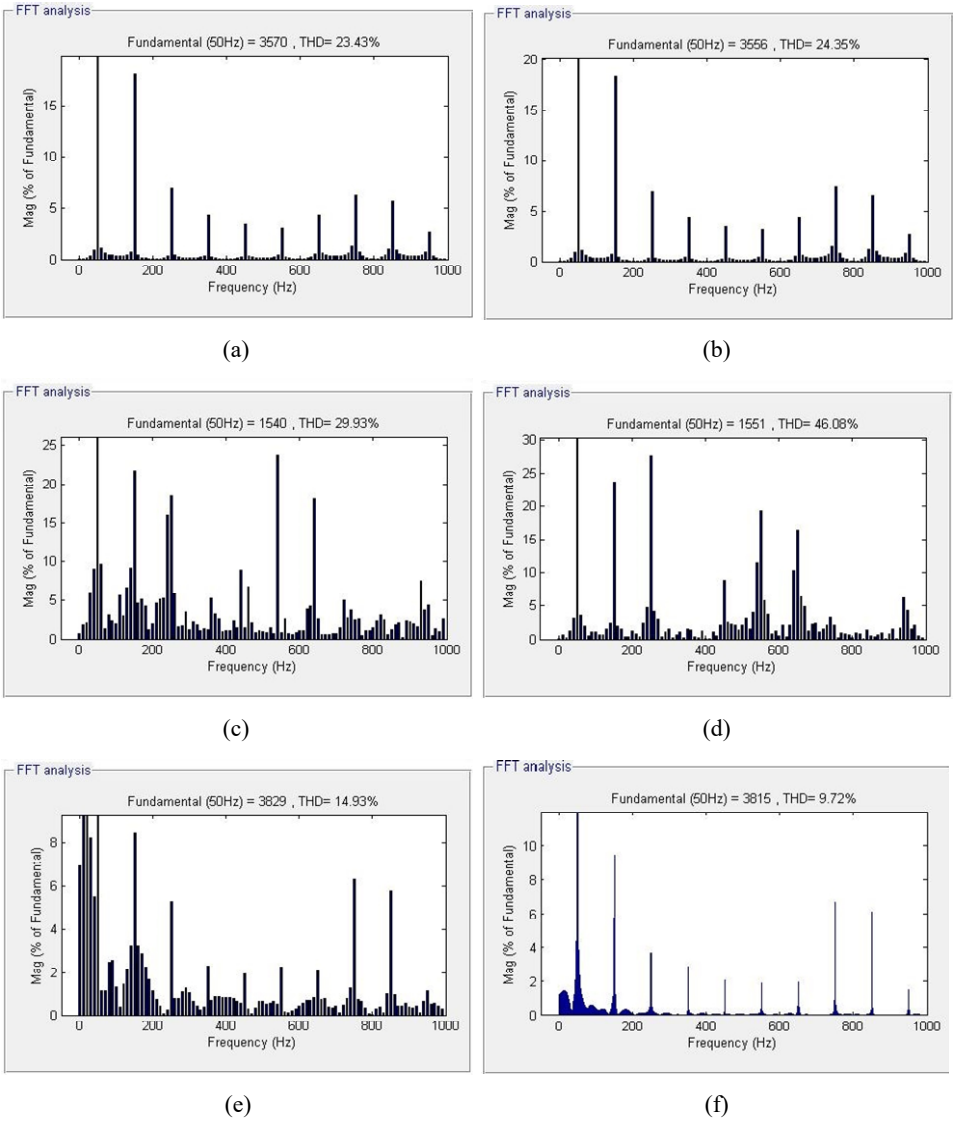

Table 4 THD for medium and high level loads of proposed MLI models

Proposed inverter configuration	*Load provided*	*Medium loads*	*High loads*
		Computed THD	*Computed THD*
Classic MLI model	R	21.65	23.43
	RL	23.96	24.35
Modified MLI model	R	16.47	29.93
	RL	33.95	46.08
Reduced switch multilevel inverter model	R	12.46	14.93
	RL	10.29	9.72

Table 5 Comparison of THD values with existing inverter models

Inverter configuration	*Load provided*	*Low loads*	*Medium loads*	*High loads*
		Computed THD	*Computed THD*	*Computed THD*
WBG inverter (Murthy-Bellur et al., 2015)	R	22.43	29.03	29.97
	RL	42.31	44.57	52.68
Distribute auxiliary inverter (Chen et al., 2015)	R	21.98	28.66	28.84
	RL	34.98	40.98	50.99
Multilevel DC/AC traction inverter (Youssef et al., 2015)	R	21.77	26.32	27.36
	RL	33.68	40.32	50.61
Traction inverter with SiC module (Nakanishi et al., 2018)	R	20.63	25.01	26.85
	RL	33.29	38.67	49.05
Inverter system (Namiki et al., 2018)	R	19.70	24.97	26.09
	RL	30.65	36.49	48.79
Modified class E inverter (Sooraj and Febin Daya, 2018)	R	19.22	24.61	25.73
	RL	32.67	36.58	48.57
Traction inverter (Chen and Ge, 2018)	R	19.03	24.55	25.67
	RL	31.27	34.90	47.90
250 kW silicon carbide MOSFET based three-level traction inverter (Wang et al., 2018)	R	18.79	23.91	24.99
	RL	30.82	34.46	47.69
Space vector modulation based transistor clamped H-bridge inverter (Jayal and Bhuvaneswari, 2021)	R	17.91	22.71	23.96
	RL	30.68	34.21	47.33
Classic MLI model	R	17.49	21.65	23.43
	RL	24.35	23.96	24.35
Proposed modified MLI model	R	12.78	16.47	29.93
	RL	29.93	33.95	46.08
Proposed reduced switch multilevel inverter model	R	9.66	12.46	14.93
	RL	11.55	10.29	9.72

4.3 Comparative analysis with existing techniques for power train models

This section of the paper provides a comparative analysis on the THD of the proposed MLI models as applicable for traction and heavy vehicle applications. Basically, there exists various forms of inverters including MLIs, auxiliary inverters, WBG inverters, class E inverter, SiC inverters, space vector modulation based H-bridge inverter and the proposed modified MLI and reduced switch MLI are compared with these inverters (Murthy-Bellur et al., 2015; Chen et al., 2015; Youssef et al., 2015; Nakanishi et al., 2018; Namiki et al., 2018; Sooraj and Febin Daya, 2018; Chen and Ge, 2018; Wang et al., 2018; Jayal and Bhuvaneswari, 2021) in respect of the THD values. The comparison is done for the same forms of low, medium and high loads given to the developed MLI

models and that of the compared existing inverter models employed for various traction applications. Table 5 confirms the superiority of the proposed reduced switch MLI model with respect to minimal THD value than the other compared models, classic MLI and modified MLI model. The effectiveness of the new reduced switch MLI model is due to the minimised numbers of switches and thereby the decrease in the THD metrics. Appendix presents the inverters employed for carrying out the experimentation process and evaluating the THD values for various load conditions.

5 Conclusions

Novel MLIs for traction and heavy vehicle applications are modelled and implemented in this research study and has been proven to be effective compared to previous inverter models form existing works pertaining to the evaluated THD value. The proposed modified MLI and reduced switch inverter model were designed and simulated for various low, medium and high loads. The classic MLI possesses a moderate level of THD value compared to Modified multilevel inverter. For loads up to 10 W, the THD values remain minimal, about 17.5%. But for higher voltage levels, the THD increases in a larger manner. Reduced switch MLIs proves to be rendering lower THD compared to the other two configurations and that compared from previous works. This reduced switch inverter can also be designed to mimic a modular inverter circuit.

To increase or decrease the output levels, the auxiliary circuit requires to be altered and employed so as to be suited for varied applications. The main difficulties arising when using such a reduced switch topology is that the design of DC link circuit and the unequal voltage stress experienced by the switches. Similar comparisons are made for higher levels of output voltages, for different inverter configurations. The filter requirement varies for these configurations, hence when unified filter is designed for multiple configurations; it is possible to develop a modular inverter topology with multiple output characteristics and is more suited for traction and heavy vehicle applications.

References

Almakhles, D.J., Ali, J.S.M., Padmanaban, S., Bhaskar, M.S., Subramaniam, U. and Sakthivel, R. (2020) 'An original hybrid multilevel DC-AC converter using single-double source unit for medium voltage applications: hardware implementation and investigation', in *IEEE Access*, Vol. 8, pp.71291-71301, DOI: 10.1109/ACCESS.2020.2986932.

Anjali Krishna, R. and Padma Suresh, L. (2016) 'A brief review on multi level inverter topologies', *International Conference on Circuit Power and Computing Technologies [ICCPCT]*.

António-Ferreira, A., Collados-Rodríguez, C. and Gomis-Bellmunt, O. (2018) 'Modulation techniques applied to medium voltage modular multilevel converters for renewable energy integration: a review', *Electric Power Systems Research*, Vol. 155, No. 1, pp.21–39.

Anwar, S., Costinett, D., Mukherjee, S. and Chowdhury, S. (2020) 'Control of SiC based integrated DC-DC powertrain charger for electric vehicles', in *2020 IEEE Energy Conversion Congress and Exposition (ECCE)*, IEEE, October, pp.4104–4111.

Blaabjerg, F., Wang, H., Vernica, I., Liu, B. and Davari, P. (2020) 'Reliability of power electronic systems for EV/HEV applications', *Proceedings of the IEEE*, Vol. 109, No. 6, pp.1060–1076.

Chen, J., Wang, L., Diao, L., Du, H. and Liu, Z. (2015) 'Distributed auxiliary inverter of urban rail train – load sharing control strategy under complicated operation condition', *IEEE Transactions on Power Electronics*, Vol. 31, No. 3, pp.2518–2529.

Chen, L. and Ge, B. (2018) 'High power traction inverter design and comparison for electric vehicle', in *2018 IEEE Transportation Electrification Conference and Expo (ITEC)*, IEEE, June, pp.583–588.

Choi, J.W. and Sul, S.K. (1996) 'Inverter output voltage synthesis using novel dead time compensation', *IEEE Trans. Power Electron.*, March, Vol. 11, No. 2, pp.221–227.

Choi, W., Lee, W., Han, D. and Sarlioglu, B. (2018) 'New configuration of multifunctional grid-connected inverter to improve both current-based and voltage-based power quality', in *IEEE Transactions on Industry Applications*, November-December, Vol. 54, No. 6, pp.6374–6382.

Desai, P.H., Bartolucci, S., Fatema, M. and Weiss, R. (2012) *Power Modules and Inverter Evaluation for GM Electrification Architectures (No. 2012-01-0340)*, SAE Technical Paper.

Dong, H., Yuan, S., Han, Z., Ding, X., Ma, S. and Han, X. (2018) 'A comprehensive strategy for power quality improvement of multi-inverter-based microgrid with mixed loads', in *IEEE Access*, Vol. 6, No. 3, pp.30903–30916.

Dorn-Gomba, L., Guo, J. and Emadi, A. (2019) 'Multi-source inverter for power-split hybrid electric powertrains', *IEEE Transactions on Vehicular Technology*, Vol. 68, No. 7, pp.6481–6494.

Drobnik, J. and Jain, P. (2013) 'Electric and hybrid vehicle power electronics efficiency, testing and reliability', *World Electric Vehicle Journal*, Vol. 6, No. 3, pp.719–730.

Feng, W., Ding, H., Chen, F., Lee, S., Chen, K., Jahns, T. and Sarlioglu, B. (2021) 'Design of high power density 100 kW surface permanent magnet machine with no heavy rare earth material using current source inverter for traction application', in *2021 IEEE Transportation Electrification Conference & Expo (ITEC)*, IEEE, June, pp.1–6.

Gopi, C. and Babu, V.R. (2021) 'Control of inverters used for axial flux induction motor based electric vehicles', in *2021 5th International Conference on Intelligent Computing and Control Systems (ICICCS)* IEEE, May, pp.603–607.

Guha, A. and Narayanan, G. (2018) 'Impact of dead time on inverter input current, DC-link dynamics, and light-load instability in rectifier-inverter-fed induction motor drives', *IEEE Transactions on Industry Applications*, March-April, Vol. 54, No. 2, pp.1414–1424.

Hinago, Y. and Koizumi, H. (2010) 'A single-phase multilevel inverter using switched series/ parallel DC voltage sources', *IEEE Trans. Ind. Electron.*, August, Vol. 57, No. 8, pp.2643–2650.

Javvaji, H.L. and Basavaraja, B. (2013) 'Simulation & analysis of different parameters of various levels of cascaded H bridge multilevel inverter', *2013 IEEE Asia Pacific Conference on Postgraduate Research in Microelectronics and Electronics (PrimeAsia)*.

Jayal, P. and Bhuvaneswari, G. (2021) 'A novel space vector modulation-based transistor-clamped H bridge inverter-fed permanent magnet synchronous motor drive for electric vehicle applications', *International Transactions on Electrical Energy Systems*, Vol. 31, No. 3, p.e12789.

Jeschke, S., Hirsch, H., Trautmann, M., Bärenfänger, J., Maarleveld, M., Obholz, M. and Heyen, J. (2016) 'EMI measurement on electric vehicle drive inverters using a passive motor impedance network', in *2016 Asia-Pacific International Symposium on Electromagnetic Compatibility (APEMC)*, IEEE, May, Vol. 1, pp.292–294.

Ji, L., Liao, C., Wang, L. and Li, S. (2018) 'An inverter for wireless charging system of electric vehicle in wide load range', *Transactions of China Electrotechnical Society*, Vol. 33, pp.9–17.

Krim, Y., Almaksour, K., Caron, H., Letrouvé, T., Saudemont, C., Francois, B. and Robyns, B. (2020) 'Comparative study of two control techniques of regenerative braking power recovering inverter based DC railway substation', in *2020 22nd European Conference on Power Electronics and Applications (EPE'20 ECCE Europe)*, IEEE, September, pp.1–9.

Kumar, B., Panigrahi, B.P. and Panda, A.K. (2015) 'Optimized level in 1-phase and 3-phase cascaded multilevel inverter using simplified technique', in *2015 International Conference on Energy, Power and Environment: Towards Sustainable Growth (ICEPE)*, IEEE, June, pp.1–5.

Kumar, P., Mishra, M., Tamang, C.K., Iqubal, A., Mishra, A., Sharma, A., Gangully, A. and Das, S. (2015) 'Performance assessment of different single phase multi-level inverter', *Michael Faraday IET International Summit: MFIIS-2015N*.

Li, X., Li, D., Chang, G., Gong, W., Packwood, M., Pottage, D., Wang, Y., Luo, H. and Liu, G. (2021) 'High-voltage hybrid IGBT power modules for miniaturization of rolling stock traction inverters', *IEEE Transactions on Industrial Electronics*, Vol. 69, No. 2, pp.1266–1275.

Luniewski, P. and Jansen, U. (2007) 'Benefits of system-oriented IGBT module design for high power inverters', in *2007 European Conference on Power Electronics and Applications*, IEEE, September, pp.1–10.

Murthy-Bellur, D., Ayana, E., Kunin, S., Palmer, B. and Varigonda, S. (2015) 'WBG inverter for commercial power generation and vehicle electrification', in *2015 IEEE International Workshop on Integrated Power Packaging (IWIPP)*, IEEE, May, pp.36–39.

Nagalakshmi, N., Ramesh Babu, U., Ali, S.M. and Sudheer, K. (2017) 'A single phase nine level inverter with reduced switches', *2017 IEEE International Conference on Power, Control, Signals and Instrumentation Engineering (ICPCSI)*.

Nakanishi, M., Hayashi, K., Enomoto, A., Hayashiguchi, M., Ando, M., Ino, K., Felgemacher, C., Mashaly, A. and Richard, G. (2018) 'Automotive traction inverter utilizing SIC power module', in *PCIM Europe 2018; International Exhibition and Conference for Power Electronics, Intelligent Motion, Renewable Energy and Energy Management*, VDE, June, pp.1–6.

Namiki, K., Murota, K. and Shoji, M. (2018) *High Performance Motor and Inverter System for a Newly Developed Electric Vehicle (No. 2018-01-0461)*, SAE Technical Paper.

Patil, R.M., Dhote, V.P. and Thosar, A. (2018) 'Comparative analysis of three phase 5, 7 9 level inverter using PDPWM technique', *2018 International Conference on Smart Electric Drives and Power System (ICSEDPS)*, Nagpur, pp.323–328.

Rashid, M.H. (2004) *Power Electronics Circuits Devices and Applications*, Pearson/Prentice-Hall, New Delhi.

Schwalbe, U. and Schilling, M. (2015) 'Topology comparison and system optimization for a modular 25 kW motor-inverter drive train system', in *Proceedings of PCIM Europe 2015; International Exhibition and Conference for Power Electronics, Intelligent Motion, Renewable Energy and Energy Management*, VDE, May, pp.1–8.

Schweikert, C., Zachariae, J., Benning, T.A. and Singh, R. (2021) 'AirSiC – a silicon-carbide based air-cooled traction inverter is the enabler for a simplified, distributed powertrain system in a passenger vehicle', in *PCIM Europe digital days 2021; International Exhibition and Conference for Power Electronics, Intelligent Motion, Renewable Energy and Energy Management*, VDE, May, pp.1–10.

Shen, Z. and Jiang, D. (2019) 'Dead-time effect compensation method based on current ripple prediction for voltage-source inverters', in *IEEE Transactions on Power Electronics*, Vol. 34, No. 1, pp.971–983, January, DOI: 10.1109/TPEL.2018.2820727.

Sooraj, V. and Febin Daya, J.L. (2018) 'Modified class E inverter based IPT system for wireless EV charging', in *2018 37th FISTA World Automotive Congress*, pp.1164–1171.

Sun H-X., Zhang H-S. and Jing Y-W. (2016) 'Tolerant control strategy for 3H bridge inverter short circuit fault of electric vehicle integrated drive system', *Electrical Machines and Control*, Vol. 20, No. 11, pp.107–116.

Suresh, Y. and Panda, A.K. (2013) 'Investigation on hybrid cascaded multilevel inverter with reduced dc sources', *Renewable and Sustainable Energy Reviews*, Vol. 26, No. 2, pp.49–59.

Wang, H., Liu, Z., Yin, S., Meng, D. and Chang, Y. (2017) 'Auxiliary inverter of urban rail train – oscillation suppression method of induction motor load', in *International Conference on Electrical and Information Technologies for Rail Transportation*, Springer, Singapore, October, pp.379–386.

Wang, L., Lam, C. and Wong, M. (2018) 'Analysis, control, and design of a hybrid grid-connected inverter for renewable energy generation with power quality conditioning', in *IEEE Transactions on Power Electronics*, August, Vol. 33, No. 8, pp.6755–6768.

Wang, S. and Lehn, P.W. (2021) 'A 3-phase electric vehicle charger integrated with dual inverter drive', *IEEE Transactions on Transportation Electrification*, Vol. 8, No. 1, pp.82–97.

Wang, Z., Mahmud, M.H., Uddin, M.H., McPherson, B., Sparkman, B., Zhao, Y., Mantooth, H.A. and Fraley, J.R. (2018) 'A compact 250 kW silicon carbide MOSFET based three-level traction inverter for heavy equipment applications', in *2018 IEEE Transportation Electrification Conference and Expo (ITEC)*, IEEE, June, pp.1129–1134.

Wu, Q., Wang, M., Zhou, W., Lu, X., Xiao, K., Bhat, K.P. and Chen, C. (2020) 'Traction inverter highly accelerated life testing with high-temperature stress', *IEEE Transactions on Transportation Electrification*, Vol. 7, No. 1, pp.304–316.

Wu, Z., Depernet, D. and Espanet, C. (2010) 'Optimal design of electrical drive and power converter for hybrid electric powertrain', in *2010 IEEE Vehicle Power and Propulsion Conference*, IEEE, September, pp.1–8.

Xiu-Juan, M., Min, Z., Yu-de, S. and Jia-Yu, W. (2008) 'A new high frequency link inverter on vehicle', in *2008 IEEE Vehicle Power and Propulsion Conference*, IEEE, September, pp.1–6.

Yamaguchi, N., Rokkaku, K. and Minami, S. (2017) 'On key issues in the spread of hybridized heavy-duty vehicles', *Journal of Asian Electric Vehicles*, Vol. 15, No. 1, pp.1767–1774.

Ye, X., Liu, W. and Lou, Y. (2017) 'Optimal design of inverter feedback device for urban rail traction power supply system', in *IECON 2017-43rd Annual Conference of the IEEE Industrial Electronics Society*, IEEE, pp.3895–3900.

Youssef, M.Z., Woronowicz, K., Aditya, K., Azeez, N.A. and Williamson, S.S. (2015) 'Design and development of an efficient multilevel DC/AC traction inverter for railway transportation electrification', *IEEE Transactions on power Electronics*, Vol. 31, No. 4, pp.3036–3042.

Zhang, F., Zhang, L., Liang, S., Sun, L. and Dai, X. (2021) 'Replacement scheme of drive boards for traction inverter module of Beijing DKZ31 metro vehicle', in *Journal of Physics: Conference Series*, February, Vol. 1754, No. 1, p.012161, IOP Publishing.

Zhang, G., Tian, Z., Tricoli, P., Hillmansen, S., Wang, Y. and Liu, Z. (2019) 'Inverter operating characteristics optimization for DC traction power supply systems', *IEEE Transactions on Vehicular Technology*, Vol. 68, No. 4, pp.3400–3410.

Zhong, Z., Wang, X., Lin, S., Fang, X., Yang, Z. and Lin, F. (2018) 'A novel control method to prevent regenerative braking failure and minimize loss of system based on supercapacitor series connected to the traction inverter', *Computers in Railways XVI: Railway Engineering Design and Operation*, Vol. 181, p.87, WIT Press, Hampshire, England, UK.

Appendix

Hardware configuration of switches employed for designed MLI models for traction and heavy vehicle application

Inverter model	*Switches*	*Voltage source*
Classic multi-level inverter	S1, S2, S3, S4 – IRG4BC20SD-PBF (600 V/10 A S-type planar IGBT)	V1, V2, V3 and V4 – 12 V
	S5, S6, S7 and S8 – IRG4BC20SD-PBF (600 V/10 A S-type planar IGBT)	
	S9, S10, S11, S12 – IRG4BC20SD-PBF (600 V/10 A S-type planar IGBT)	
	S13, S14, S15, S16 – IRG4BC20SD-PBF (600 V/10 A S-type planar IGBT)	
Proposed modified multi-level inverter model	S1, S2, S3, S4 – IRG4BC20SD-PBF (600 V/10 A S-type planar IGBT)	V1-12 V
	S5, S6, S7 and S8 – IRG4BC20SD-PBF (600 V/10A S-type planar IGBT)	V2-18 V
Proposed reduced switch multi-level inverter model	S1, S2, S3, S4 – FID50-12BD (1,200 V/50 A Bidirectional Switch with IGBT and fast diode bridge)	V1, V2, V3 and V4 – 12V
	S5, S6 and S7 – IRG4BC20SD-PBF (600 V/10A S-type planar IGBT)	